Quantum switches and quantum memories for matter-wave lattice solitons

2007 New J. Phys. 9 4

(http://iopscience.iop.org/1367-2630/9/1/004)

New Journal of Physics
The open–access journal for physics

Quantum switches and quantum memories for matter-wave lattice solitons

V Ahufinger[1], A Mebrahtu[2], R Corbalán[3] and A Sanpera[4]

[1] ICREA and Grup d'Òptica, Departament de Física, Universitat Autònoma de Barcelona, E-08193 Bellaterra, Barcelona, Spain
[2] Institut für Theoretische Physik, Universität Hannover, D-30167 Hannover, Germany
[3] Grup d'Òptica, Departament de Física, Universitat Autònoma de Barcelona, E-08193 Bellaterra, Barcelona, Spain
[4] ICREA and Grup de Física Teòrica, Departament de Física, Universitat Autònoma de Barcelona, E-08193 Bellaterra, Barcelona, Spain
E-mail: sanpera@ifae.es

New Journal of Physics **9** (2007) 4
Received 4 September 2006
Published 17 January 2007
Online at http://www.njp.org/
doi:10.1088/1367-2630/9/1/004

Abstract. We study the possibility of implementing a quantum switch and a quantum memory using matter-wave lattice solitons and making them interact with 'effective' potentials (barrier/well) corresponding to defects of the optical lattice. In the case of interaction with an 'effective' potential barrier, the bright lattice soliton experiences an abrupt transition from complete transmission to complete reflection (quantum switch) for a critical height of the barrier. The trapping of the soliton in an 'effective' potential well and its release on demand, without losses, shows the feasibility of using the system as a quantum memory. The inclusion of defects as a way of controlling the interactions between two solitons is also reported.

PII: S1367-2630(07)32081-8

Contents

1. Introduction

Bose–Einstein condensates (BEC) in optical lattices have attracted during recent years a lot of attention both in the mean field regime (for recent reviews see for instance [1]) as well as in the strongly correlated regime (for recent reviews see for instance [2]). One of the main reasons for this activity burst is the high level of control achieved in the experiments of ultracold gases in optical lattices which permits one to explore a broad range of fundamental phenomena.

In the mean field regime, huge interest has been devoted to nonlinear dynamics of matter-waves in periodic media and specifically to matter-wave solitons. Matter-wave solitons are self-stabilized coherent atomic structures that appear in nonlinear systems due to the balance between the nonlinearity and the dispersive effects. The nature of the solitons supported by BEC is determined by the character of the interactions: attractive (repulsive) nonlinearity supports bright [3] (dark [4]) solitons. In the presence of an optical lattice, this scenario changes completely due to the appearance of a band structure in the spectrum and the possibility of having either bright or dark lattice solitons with either repulsive or attractive interactions arises. Very recently, the first experimental demonstration of bright lattice solitons in repulsive condensates was reported [5].

Since the first proposals of BEC lattice solitons [6], there has been an explosion of contributions regarding generation, mobility and interactions of these novel types of matter-wave solitons both in one-dimensional (1D) systems [7]–[9] and in higher dimensions [10]. The interest is mainly centred on bright matter-wave lattice solitons due to their potential applications in energy and information transport without losses. The fact that matter-wave solitons are massive permits one to generate them at rest and to move them after an appropriate transfer of momentum. Proposals to control the dynamics of bright gap solitons are mainly devoted either to manipulate the optical lattice [11] or to modify the nonlinearity [12]. Nevertheless, a complete control on the dynamics of bright matter-wave gap solitons also requires a profound knowledge of their interactions with defects.

The interaction of solitons with local inhomogeneities is a subject that appears in the literature in different contexts and has been studied in the framework of different nonlinear equations (see for instance [13]). In particular, the nonlinear Schrödinger equation with point-like defects either in the continuum regime [14] or in discrete systems [15] has deserved special attention. Extended defects have also been addressed in this framework [16]. In nonlinear optics, the coupled mode equations have been used to study collisions of moving Bragg solitons with

finite size [17, 18] and point-like defects [19]. Very recently, interactions with defects in the context of continuous matter-wave solitons have also been addressed [20, 21].

In this paper, we focus on bright lattice matter-wave solitons and propose different possibilities to control their dynamics through interactions with defects of arbitrary amplitude and width. Specifically we will show how to reverse the direction of movement of the soliton (a complete bounce back) and how it can be stored and retrieved on demand. In section 2, the physical system considered and the model used is introduced. In section 3, we present the results concerning the interaction of solitons with an 'effective' potential barrier, where the possibility of implementing a quantum switch arises. Next, in section 4 the results regarding the interaction with an 'effective' potential well are shown and the potential use of the system as a quantum memory is discussed. The possibility of controlling the interactions between two lattice solitons by placing a defect at the interaction point is discussed in section 5. We conclude in section 6.

2. Physical system

We consider a zero temperature ^{87}Rb condensate confined in a 1D geometry and in the presence of an optical lattice. The description of the system is performed within the 1D Gross–Pitaevskii equation (GPE)

$$i\hbar \frac{d\psi(x,t)}{dt} = \left(-\frac{\hbar^2}{2m}\triangle + V(x) + g|\psi(x,t)|^2 \right) \psi(x,t), \tag{1}$$

where $g = 2\hbar a_s \omega_t$, with a_s the s-wave scattering length and ω_t the radial angular trapping frequency, is the averaged 1D coupling constant. The external potential is given by:

$$V(x) = \frac{m}{2}{\omega_x}^2 x^2 + V_0 \sin^2\left(\frac{\pi x}{d}\right), \tag{2}$$

which describes both the axial trapping potential, with angular frequency ω_x, and the optical lattice, with spatial period $d = \lambda/2\sin(\theta/2)$, λ being the wavelength of the lasers forming the optical lattice and θ the angle between them. The depth of the optical lattice, V_0, is given in units of the lattice recoil energy $E_r = \hbar^2 k^2/2m$ where $k = \pi/d$ is the lattice recoil momentum.

The generation of the bright lattice soliton is performed as is reported in [8] using parameters close to the experimental realizations [5]. The procedure is briefly summarized as follows. The starting point is a ^{87}Rb condensate ($a_s = 5.8\,\text{nm}$, $m = 1.45 \times 10^{-25}\,\text{Kg}$) of $N = 500$ atoms in the presence of a magnetic trap with frequencies $\omega_t = 715 \times 2\pi\,\text{Hz}$ and $\omega_x = 14 \times 2\pi\,\text{Hz}$ and an optical lattice with potential depth $V_0 = 1E_r$ and period $d = 397.5\,\text{nm}$. The axial magnetic trap is suddenly turned off and an appropriate phase imprinting, corresponding to phase jumps of π in adjacent sites, is performed [8]. After the phase imprinting, the system evolves towards a negative mass self-maintained staggered soliton at rest centred at $x = 0$, which contains approximately 35% of the initial atoms ($N = 187$) and extends circa 11 sites. The excess atoms are lost by radiation.

The total energy of the generated bright lattice soliton can be calculated using the energy functional of the GPE (1) that contains the total kinetic ($E_{\mathrm{k}}^{\mathrm{T}}$), interaction ($E_{\mathrm{i}}$) and potential ($E_{\mathrm{p}}$) energies

$$E = \int \left[\frac{\hbar^2}{2m} |\nabla \psi(x)|^2 + \frac{g}{2} |\psi(x)|^4 + V(x) |\psi(x)|^2 \right] \mathrm{d}x. \tag{3}$$

As can be observed in the numerical solutions of the GPE, the density profile of the bright lattice soliton inside each well is shifted with respect to the minimum of the optical lattice. This shift has to be taken into account to properly calculate the energy. Considering a Gaussian ansatz for a soliton at rest, centred at $x = 0$ and with amplitude A, $\psi(x) = A \exp(-(x - x_0)^2/2\eta^2) \cos(2\pi x/(\lambda'))$, with $\lambda' = 2d + \delta$ and η the width [9], the energy functional reads

$$\begin{aligned} E = B\Bigg(\frac{\hbar^2}{m} \left[\frac{1 + \mathrm{e}^{-k'^2\eta^2} \cos(2k'x_0)}{2\eta^2} + k'^2 \right] + \frac{g|A|^2}{4\sqrt{2}} \Big[3 + \mathrm{e}^{-2k'^2\eta^2} \cos(4k'x_0) \\ + 4\mathrm{e}^{-\frac{k'^2\eta^2}{2}} \cos(2k'x_0) \Big] + V_0 \Big[1 + \mathrm{e}^{-k'^2\eta^2} \cos(2k'x_0) - \mathrm{e}^{-k^2\eta^2} \cos(2kx_0) \\ - \tfrac{1}{2}\mathrm{e}^{-k_-^2\eta^2} \cos(2k_-x_0) - \tfrac{1}{2}\mathrm{e}^{-k_+^2\eta^2} \cos(2k_+x_0) \Big] \Bigg). \end{aligned} \tag{4}$$

where $B = |A|^2\sqrt{\pi}\eta/4$, $k' = 2\pi/\lambda'$ and $k_\pm = k' \pm k$. We demand normalization of the wave function ansatz and fixing $N = 187$, $\delta = 0.07\,\mu$m and $x_0 = 0$, we obtain a minimum of equation (4) corresponding to $1.31E_{\mathrm{r}}$. Exact numerical integration of equation (3) gives a total energy of $1.35E_{\mathrm{r}}$. This shows the high level of accuracy that the used variational method provides. Also, a close agreement is found when we evaluate separately each term of equation (3) by using the variational method [9] (exact integration): $E_{\mathrm{k}}^{\mathrm{T}} = 0.85E_{\mathrm{r}}(0.85E_{\mathrm{r}})$, $E_{\mathrm{i}} = 0.12E_{\mathrm{r}}(0.13E_{\mathrm{r}})$ and $E_{\mathrm{p}} = 0.34E_{\mathrm{r}}(0.37E_{\mathrm{r}})$.

By calculating the linear band spectrum of the system, we obtain an energy at the band edge of $1.25E_{\mathrm{r}}$. This value is in good agreement with the total energy obtained previously (equation (3)) without the nonlinear term. The linear band spectrum predicts an effective mass at the edge of the first Brillouin zone corresponding to $m_{\mathrm{eff}} = -0.15m$.

Once the lattice soliton is created, it is set into motion by applying an instantaneous transfer of momentum at $t = 0$. It has to be large enough to overcome the Peierls–Nabarro (PN) barrier [8, 22] but sufficiently small to assure that the soliton remains in the region of negative effective mass, i.e., $0.009k\hbar < p < 0.2k\hbar$. The soliton starts to move opposite to the direction of the kick, manifesting thus its negative effective mass. The concept of the effective mass is used through the paper to give an intuitive explanation of the observed dynamics. Nevertheless, all the results presented in what follows have been obtained, without any approximation, by direct integration of equation (1).

At a certain distance x_{m} of the initial position of the soliton ($x = 0$), the lattice potential $V(x)$ is modified in the following way

$$\begin{cases} V_0 \sin^2\left(\dfrac{\pi x}{d}\right) + V_{\mathrm{m}} \left(1 - \dfrac{(x - x_{\mathrm{m}})^2}{2\sigma^2}\right) & \text{if } x_m - l/2 \leqslant x \leqslant x_m + l/2; \\ V_0 \sin^2\left(\dfrac{\pi x}{d}\right) & \text{otherwise.} \end{cases} \tag{5}$$

where V_m can be either positive or negative and $\sigma = 6d$ for all the cases. For $V_m < 0$, the local decrease of the lattice potential corresponds to an 'effective' potential barrier for the soliton due to its negative effective mass while if $V_m > 0$, i.e. a local increase of the potential acts as an 'effective' well for the soliton. In the case of an effective barrier, x_m is fixed to match exactly a minimum of the optical lattice, while in the effective well case, x_m corresponds to a maximum of the optical lattice. We have checked that the results reported in the following do not depend strongly on the specific shape of the defect by reproducing them with Gaussian and square profiles also.

To analyse the interaction of the bright lattice soliton with the defect, it is crucial to know the total energy of the soliton while it moves. The applied variational ansatz with the shift in the periodicity is meaningful only in the static case and cannot be used to study soliton dynamics, since the soliton is always chirped with respect to its centre [9]. Therefore, to study dynamical behaviour one has to rely on numerical simulations. We have numerically calculated the contributions to the total energy of the soliton as a function of time. Immediately after the kick, the soliton expels atoms and its energy abruptly decreases becoming much smaller than the energy that it would need to remain at rest at the edge of the first Brillouin zone. In the framework of the linear band theory, this would correspond to displacing the particle from the edge of the band of the first Brillouin zone by changing its quasimomentum. To illustrate the dynamics of the system, we consider the case in which we give a kick of $p = 0.1k\hbar$ to the generated soliton at rest. At $t = 0$, just after the kick, the total energy of the soliton corresponds to its energy at rest plus the contribution due to the transfer of momentum, i.e. $E = 1.35E_r + (0.1)^2 E_r = 1.36E_r$. At $t = 1$ ms, the soliton energy has decreased already to $0.96E_r$, the rest of the energy has been taken by the expelled atoms. A steady state is reached for a soliton energy of $E = 0.92E_r$. While moving, some energy is devoted to cross the PN barrier (the soliton configuration changes its shape from a configuration centred in one well of the optical lattice to a configuration centred in one maximum and vice versa). This change of the shape of the soliton is reflected in the out of phase oscillations of the kinetic energy with respect to the potential plus nonlinear energy in such a way that the mean value of the energy remains constant.

3. 'Effective' potential barrier

We discuss first the interaction of a bright lattice soliton with an 'effective' potential barrier. Scattering depends on the width of the defect l and the relevant energy scale, settled by the ratio $|V_m|/E_k$, where $E_k = \langle P \rangle^2/2m$ is the fraction of the total kinetic energy E_k^T devoted to move the soliton, and $\langle\ \rangle$ denotes the time average (before reaching the defect). The momentum P is defined as

$$P(t) = \int -i\hbar\psi^*(x, t)\nabla\psi(x, t)\, dx. \tag{6}$$

The remaining kinetic energy is needed to keep the solitonic structure and cannot be used to overcome the 'effective' potential barrier. We have checked that apart from the necessary change in shape to overcome the PN barrier, the soliton keeps its overall shape when it reaches the defect. This corroborates that there is no transfer between nonlinear energy and kinetic energy apart of the one corresponding to the already discussed PN barrier.

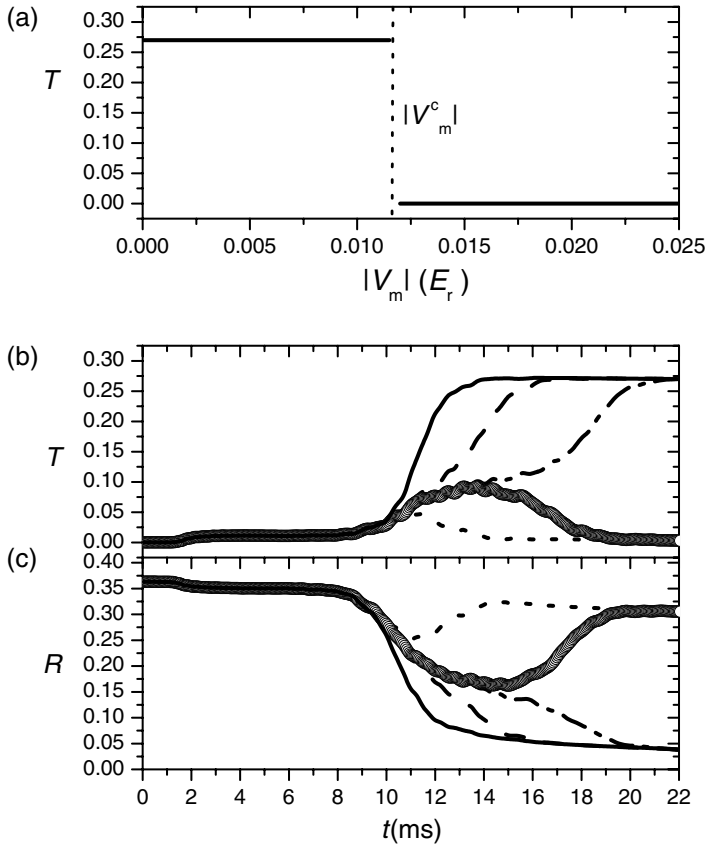

Figure 1. (a) Transmission coefficient, T, as a function of the amplitude of the 'effective' potential barrier, $|V_m|$; (b) transmission coefficient, T, and (c) reflection coefficient, R, as a function of time for different amplitude defects: $|V_m| = 0$ (solid line), $|V_m| = 0.01E_r$ (dashed line), $|V_m| = 0.0115E_r$ (dot-dashed line), $|V_m| = 0.0117E_r$ (circles) and $|V_m| = 0.018E_r$ (dotted line). In all the plots, the soliton kinetic energy is $E_k = 0.01E_r$ and the width of the defect $l = 2d$.

We distinguish two regimes of parameters: (i) when the amplitude of the 'effective' potential barrier is on the order of the kinetic energy of the soliton ($|V_m| \sim E_k$) and (ii) when the amplitude of the potential barrier is much larger than the kinetic energy of the soliton. In the former case, the potential barrier acts as a quantum switch, i.e., either the entire soliton is transmitted or it is completely reflected depending on the amplitude of the barrier (figure 1(a)). The transmission (T) and reflection (R) coefficients are calculated by integrating over space (and time) the density of the wavefunction in the region after and before the defect, respectively. Note that since only approximately 35% of the initial atoms form a soliton and since there are also losses of atoms during the kick, the merit figure for perfect transmission is well below 1 and corresponds approximately to 0.27 ($N = 135$).

For a fixed width of the defect a drastic change of behaviour occurs for a given height of the barrier $|V_m^c|$. The wider the defect the lower the critical value of the height of the barrier $|V_m^c|$. The critical values, indicating the transition between complete transmission and complete reflection for different potential widths are shown in figure 2(a) by solid black squares. Below these values, depicted by a grey region in figure 2(a), complete transmission of the soliton occurs.

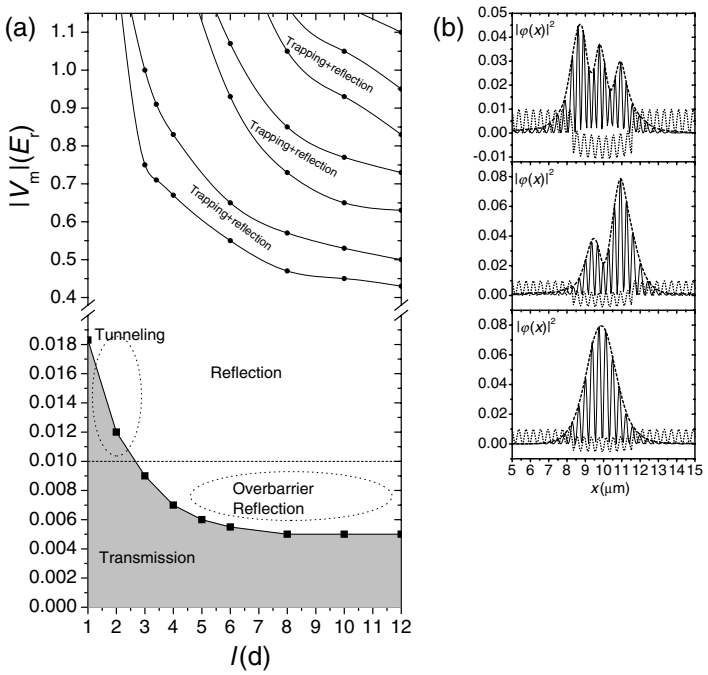

Figure 2. (a) Reflection and transmission behaviour of a soliton interacting with an effective potential barrier as a function of the potential width l (in d units) and potential amplitude $|V_m|$ (in E_r units): the region of total transmission in grey, and the region of total reflection in white. Inside the reflection region, bands in which trapping and reflection occurs appear. Region of parameters for which tunnelling and overbarrier reflection occur are also shown. The dashed line shows the value of the kinetic energy of the soliton. (b) Density profiles of the trapped structure that appears for $|V_m| = 0.55E_r$ (lower plot), $|V_m| = 0.8E_r$ (middle plot) and $|V_m| = 1.1E_r$ (upper plot). In the three cases $l = 8d$.

As one approaches the critical value from below, the soliton experiences a time delay with respect to free propagation (i.e., in the absence of the defect). This delay increases as one gets closer to the critical point and eventually the time needed by the soliton to cross the barrier diverges (see figure 3). Above the transition line, reflection of the entire soliton occurs after a storage time inside the region of the barrier that also increases as one approaches the critical value. To illustrate this behaviour, figure 1(b) and (c) show transmission and reflection coefficients as a function of time for a barrier of fixed width $l = 2d$ and different values of the amplitude. In the situation shown in figure 1, the critical value is nearly equal to the kinetic energy of the soliton but if the width of the barrier is reduced, this critical value can exceed the kinetic energy of the soliton. In this case, the soliton tunnels through the barrier, i.e., transmission is obtained for values of the amplitude of the barrier higher than the kinetic energy of the soliton (see figure 2(a)). On the other hand, for wider defects, a region of overbarrier reflection appears (figure 2(a)). There, the lattice soliton is completely reflected although it has a kinetic energy larger than the height of the potential barrier. This region extends for a wide range of widths of the defect. We have checked that overbarrier reflection occurs even in the limit when the width of the defect is much larger than the size of the soliton.

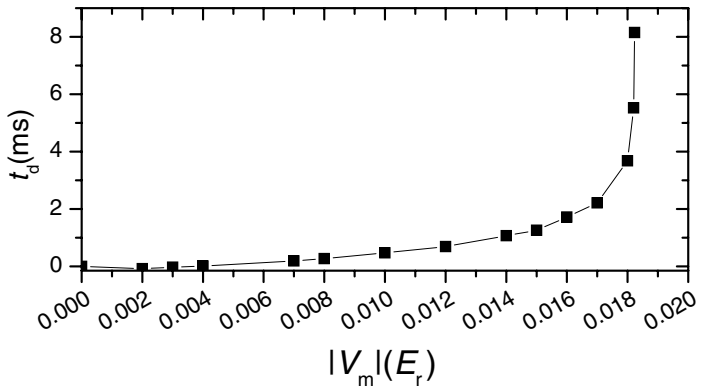

Figure 3. Transmission delay time as a function of $|V_m|$ for a soliton with kinetic energy $E_k = 0.01E_r$ crossing a defect of width $l = d$.

Figure 3 shows the delay time in transmission with respect to the absence of defect, t_d, for $l = d$ as a function of the height of the barrier, $|V_m|$, including the cases where tunnelling occurs ($|V_m| > 0.01E_r$).

Up to now we have described the transition from complete transmission to complete reflection by fixing the width of the defect and varying the amplitude. It is worth noting that a similar switching behaviour can be obtained by fixing the amplitude of the effective potential and changing its width. This would correspond to horizontal lines in figure 2(a) crossing the transition line (solid black squares) in the region where $|V_m|$ is on the order of the kinetic energy of the soliton. This observed abrupt transition from complete reflection to complete transmission opens the possibility to use the system as a quantum switch. A similar switching behaviour has been predicted for optical Bragg solitons described with the coupled mode equations [18].

Let us now focus on the regime where the amplitude of the barrier is much larger than the kinetic energy of the soliton $|V_m| \gg E_k$, and the expected behaviour is complete reflection of the soliton. Complete reflection indeed occurs but there are specific values of the ratio $l/|V_m|$ for which the soliton splits into two parts: a fraction of the initial soliton becomes trapped inside the region of the barrier while the other part is reflected back keeping a solitonic structure. Figure 2(a) shows the regions where the soliton split into two (trapping and reflection) embedded in the complete reflection region. The fraction of atoms trapped inside the defect has its origin on the atoms lost by radiation due to the repulsive force experienced by the soliton when it reaches the potential barrier. These radiated atoms enter the region of the barrier and for some specific ratios of the width and the height of the defect the fraction of trapped atoms increases. These trapping regions appear as bands as shown in figure 2(a). In each band, the trapped fraction exhibits different spatial distributions: for the first (lowest) one, the structure is a single hump; in the second one a double hump structure appears, and so on (see figure 2(b)). A noticeable feature of this trapped fraction is that the density maxima of the structure are located at the positions of the maxima of the optical potential. Increasing the amplitude of the barrier, the structure becomes more independent of the lattice periodicity. The extension of the trapped structure is the same independently of the features of the barrier but the number of trapped atoms differs for different widths of the barrier. The narrower the defect is the larger the number of trapped atoms. This number changes also with $|V_m|$ inside each band, being maximum at the centre of the band. For all cases the number of atoms forming the reflected

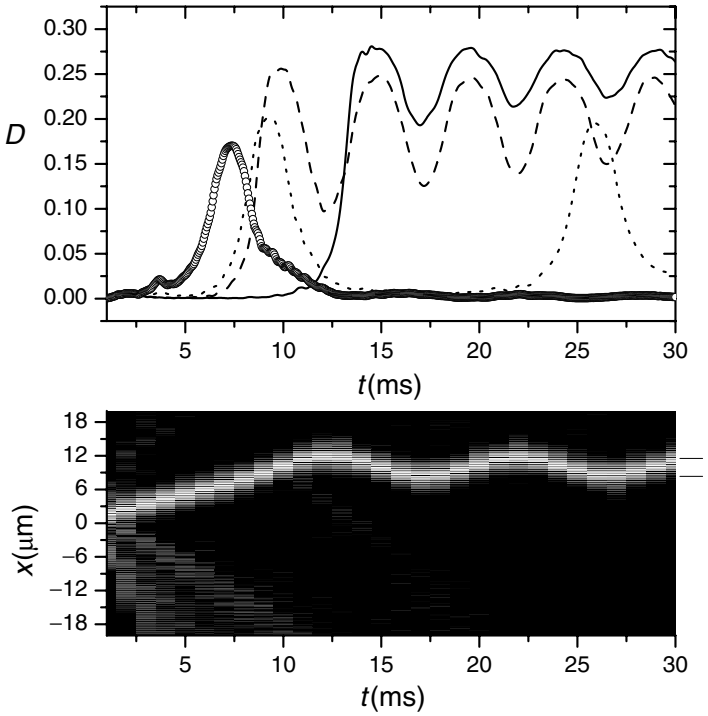

Figure 4. (a) Temporal evolution of the trapped fraction of the soliton interacting with an 'effective' well of depth $|V_m| = 0.018E_r$ and width $l = 8d$ after an instantaneous transfer of momentum of $p = 0.05k\hbar$ (solid line), $p = 0.1k\hbar$ (dashed line), $p = 0.17k\hbar$ (dotted line) and $p = 0.2k\hbar$ (circles). (b) Contour plot of the evolution in space and time of the lattice soliton with conditions corresponding to the dashed line case in (a).

soliton is always larger than the trapped fraction. We have checked that these 'resonance' bands do not correspond to bound states of the linear case. We have observed that this behaviour occurs for all the accessible initial transfers of momentum that allow motion of the soliton.

4. 'Effective' potential well

Let us now turn to the interaction of a lattice soliton with an 'effective' potential well with a depth of the order of its kinetic energy. For a fixed depth of the well, the soliton exhibits different behaviours depending on its kinetic energy. For low kinetic energies, the soliton gets bound with the defect and exhibits oscillations while for kinetic energies overcoming a certain threshold, the soliton crosses the defect region. In the latter case, the only detectable effect of the potential well is the speed-up of the soliton with respect to free propagation. It is important to note that as the width of the defect increases, the range of velocities for which transmission occurs decreases. To illustrate the described behaviour, figure 4(a) shows the time evolution of the trapped fraction density, D, for different initial transfer of momentum: $p = 0.05k\hbar$ (solid line), $p = 0.1k\hbar$ (dashed line), $p = 0.17k\hbar$ (dotted line) and $p = 0.2k\hbar$ (circles) keeping fixed the depth ($|V_m| = 0.018E_r$) and the width ($l = 8d$) of the well.

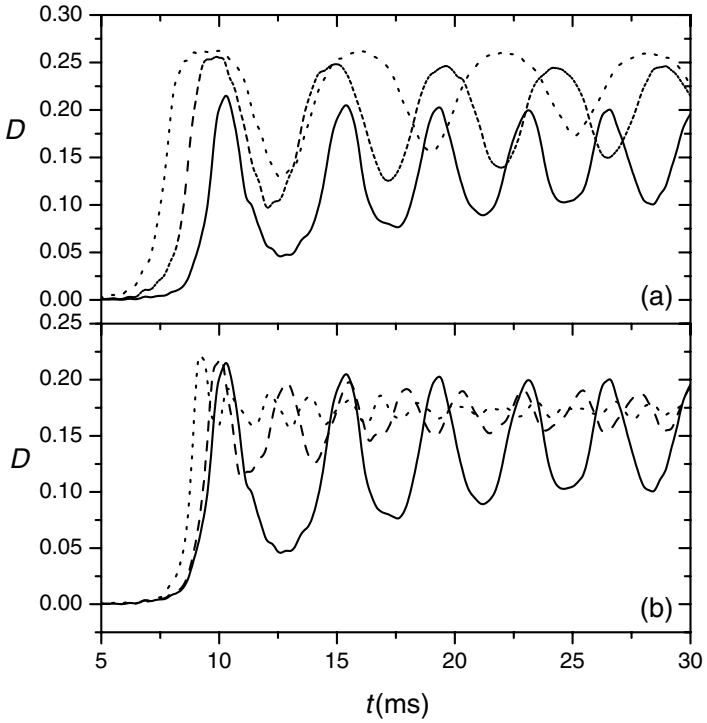

Figure 5. Temporal evolution of the trapped fraction density of a lattice soliton with $E_k = 0.01E_r$ interacting with an 'effective' well with (a) $|V_m| = 0.018E_r$ and $l = 4d$ (solid line), $l = 8d$ (dashed line) and $l = 12d$ (dotted line); (b) $l = 4d$ and $|V_m| = 0.018E_r$ (solid line), $|V_m| = 0.03E_r$ (dashed line) and $|V_m| = 0.08E_r$ (dotted line).

The minima of the trapped fraction correspond to the turning points of the oscillating movement of the soliton around the 'effective' well. The maxima indicates the times for which the soliton is completely inside the well. As expected, the amplitude of the oscillations increases with an increasing momentum transfer. If the amplitude of the oscillation is larger than the width of the defect, the turning points are located outside the potential well, indicated by a lower value of D. Figure 4(b) shows a contour plot of the evolution in space and time of a lattice soliton with $E_k = 0.01E_r$ interacting with an 'effective' well of width $l = 8d$ and depth $|V_m| = 0.018E_r$ (dashed line case in figure 4(a)). The width of the 'effective' well is shown at the right-hand part of the plot to illustrate that indeed the turning points are outside the defect.

By fixing $E_k = 0.01E_r$, we explore now the dependence of the oscillations on l and $|V_m|$. Figure 5(a) displays the temporal evolution of the trapped fraction, D, for $|V_m| = 0.018E_r$ and different values of the width of the defect: $l = 4d$ (solid line), $l = 8d$ (dashed line) and $l = 12d$ (dotted line). The frequency of the oscillations gives an indication of the width of the defect, decreasing as the width increases, while the amplitude remains approximately the same for all widths. In figure 5(b) we fix $l = 4d$ and display the trapped fraction, D, as a function of time for $|V_m| = 0.018E_r$ (solid line), $|V_m| = 0.03E_r$ (dashed line) and $|V_m| = 0.08E_r$ (dotted line). By inspection of figure 5(b), one can confirm that the frequency of the oscillations increases with the depth of the potential while the amplitude of the oscillations decreases. This is due to the fact that the soliton experiences a much larger attractive force as the depth of the defect increases limiting the displacements around the central position of the well.

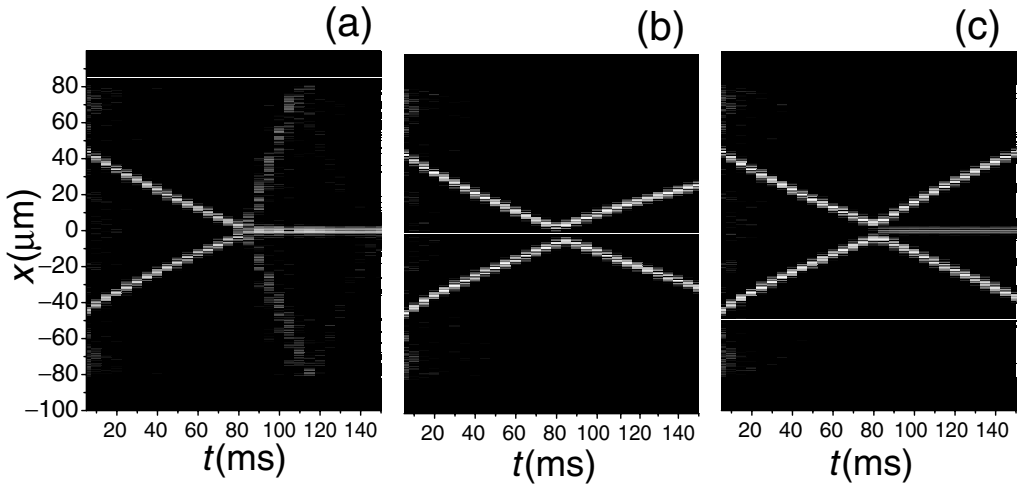

Figure 6. Contour plot of the evolution in space and time of a collision between two identical solitons initially placed at symmetrical positions with respect $x = 0$ and moving in opposite directions when an 'effective' potential barrier with $l = 2d$ and (a) $|V_m| = 0.012E_r$, (b) $|V_m| = 0.2E_r$ and (c) $|V_m| = 0.5E_r$ is placed at $x = 0$.

The trapping of the entire lattice soliton around the position of the defect opens possibilities to use the system as a quantum memory because it provides the capacity of storage. Nevertheless, in order to implement a memory, one should also be able to release the trapped structure after a desirable time and with the minimum losses. We have checked that a soliton trapped in an 'effective' potential well can be released with a certain velocity keeping the totality of its initial atoms if the defect amplitude is instantaneously set to zero. In fact the velocity of the lattice soliton after releasing it will depend on the amplitude of the oscillations it was performing while it was trapped. Specifically, the velocity of the structure, after releasing it, grows with the amplitude of the oscillations. Moreover, choosing appropriately the time at which the release takes place, one can choose the direction of the movement.

5. Control of the collisions

Now we investigate if the inclusion of a defect in the lattice helps to control the interactions between two lattice solitons. It has been shown that collision of two identical lattice solitons (moving with the same velocity and with the same average phase) merge into a soliton with the same number of atoms as the initial ones [9]. The excess atoms are lost by radiation. If an 'effective' potential barrier much narrower than the soliton's dimensions is placed at the crossing point, we find the following behaviours: (i) for $|V_m| \leqslant E_k$ the merging behaviour is maintained (figure 6(a)); (ii) for $|V_m| \gg E_k$, each soliton reflects back (figure 6(b)). Moreover, for some values of $|V_m|$, in addition to the reflection, a fraction of atoms can be trapped in the defect (figure 6(c)). The trapped fraction shows up the same features as in the single soliton case (section 3). Modifying the features of the defect, different outcomes can be engineered. For instance, when the width of the barrier is of the order of the dimensions of the initial solitons, effects like the trapping of both solitons at the edges of the barrier can occur.

6. Conclusions

Summarizing, we have found that bright matter-wave lattice solitons behave as 'quantum' particles when colliding with an 'effective' barrier/well, corresponding to a defect in the optical lattice. Among the rich dynamics exhibited by the system, we would like to remark on two effects. The first one corresponds to the interaction of a soliton with an 'effective' potential barrier which permits the implementation of a quantum switch. In this case, a sharp transition from complete reflection to complete transmission is present at a specific value of the height of the barrier. Although this resembles the classical particle behaviour, the quantum nature of the solitons is explicitly manifested in the appearance of overbarrier reflection and tunnelling. The second effect we would like to stress appears when the defect acts as an 'effective' potential well. We have shown that trapping of the entire soliton around the position of the defect and its release on demand with a given velocity and direction of motion is possible. This fact indicates the suitability of the system as a quantum memory. Finally, it has been also reported that the presence of a defect in the lattice can help to control the interactions of two lattice solitons.

Acknowledgments

We thank M Lewenstein and A Bramon for fruitful discussions. We acknowledge support from the Spanish Ministerio de Ciencia y Tecnología (FIS2005-01369, FIS2005-01497, Consolider Ingenio 2010 CSD2006-00019) and from the Catalan Government (SGR2005-00358). AM acknowledges financial support from the Deutscher Akademischer Austausch Dienst (DAAD).

References

[1] Morsch O and Oberthaler M 2006 *Rev. Mod. Phys.* **78** 179
Brazhnyi V A and Konotop V V 2004 *Mod. Phys. Lett.* B **18** 627
[2] Bloch I and Greiner M 2005 *Adv. At. Mol. Opt. Phys.* **52** 1
Lewenstein M *et al Preprint* cond-mat/0606771
[3] Khaykovich L *et al* 2002 *Science* **296** 1290
Strecker K E *et al* 2002 *Nature* **417** 150
[4] Burger S *et al* 1999 *Phys. Rev. Lett.* **83** 5198
Denschlag J *et al* 2000 *Science* **287** 97
[5] Eiermann B *et al* 2004 *Phys. Rev. Lett.* **92** 230401
[6] Zobay O *et al* 1999 *Phys. Rev.* A **59** 643
Trombettoni A and Smerzi A 2001 *Phys. Rev. Lett.* **86** 2353
[7] Abdullaev F Kh *et al* 2001 *Phys. Rev.* A **64** 043606
Louis P J Y *et al* 2003 *Phys. Rev.* A **67** 013602
Sakaguchi H and Malomed B A 2004 *J. Phys. B: Mol. Opt. Phys.* **37** 1443
Louis P J Y, Ostrovskaya E A and Kivshar Y S 2004 *J. Opt. B: Quantum Semiclass. Opt.* **6** S309
Dabrowska B J, Ostrovskaya E A and Kivshar Y S 2004 *J. Opt. B: Quantum Semiclass. Opt.* **6** 423
[8] Ahufinger V *et al* 2004 *Phys. Rev.* A **69** 053604
[9] Ahufinger V and Sanpera A 2005 *Phys. Rev. Lett.* **94** 130403
[10] Baizakov B B, Konotop V V and Salerno M 2002 *J. Phys. B: At. Mol. Opt. Phys.* **35** 5105
Ostrovskaya E A and Kivshar Y S 2003 *Phys. Rev. Lett.* **90** 160407
Baizakov B B, Malomed B A and Salerno M 2003 *Europhys. Lett.* **63** 642
Sakaguchi H and Malomed B A 2004 *J. Phys. B: Mol. Opt. Phys.* **37** 2225
Dudarev A M, Diener R B and Niu Q 2004 *J. Opt. B: Quantum Semiclass. Opt.* **6** S231

[11] Brazhnyi V A, Konotop V V and Kuzmiak V 2004 *Phys. Rev.* A **70** 043604
Louis P J Y, Ostrovskaya E A and Kivshar Y S 2005 *Phys. Rev.* A **71** 023612
Kevrekidis P G *et al* 2005 *Phys. Rev.* A **71** 023614
Porter M A *et al* 2005 *Preprint* cond-mat/0507696
Brazhnyi V A, Konotop V V and Pérez-García V M 2006 *Phys. Rev. Lett.* **96** 060403
Brazhnyi V A, Konotop V V and Pérez-García V M 2006 *Phys. Rev.* A **74** 23614
[12] Cuevas J, Malomed B A and Kevrekidis P G 2005 *Phys. Rev.* E **71** 066614
Abdullaev F Kh and Garnier J 2005 *Phys. Rev.* A **72** 061605
[13] Kivshar Y S and Malomed B A 1989 *Rev. Mod. Phys.* **61** 763
Forinash K, Peyrard M and Malomed B 1994 *Phys. Rev.* E **49** 3400
Kiselev S A, Bickham S R and Sievers A J 1994 *Phys. Rev.* B **50** 9135
Rakhmanova S and Mills D L 1998 *Phys. Rev.* B **58** 11458
Alexeeva N V, Barashenkov I V and Tsironis G P 2000 *Phys. Rev. Lett.* **84** 3053
[14] Kivshar Y S, Kosevich A M and Chubykalo O A 1987 *Phys. Lett.* A **125** 35
Pushkarov D I and Atanasov R D 1990 *Phys. Lett.* A **149** 287
Cao X D and Malomed B A 1995 *Phys. Lett.* A **206** 177
Goodman R H, Holmes P J and Weinstein M I 2004 *Physica* D **192** 215
[15] Konotop V V *et al* 1996 *Phys. Rev.* E **53** 6476
[16] Balakrishnan R 1985 *Phys. Rev.* A **32** 1144
Frauenkron H and Gassberger P 1996 *Phys. Rev.* E **53** 2823
Stoychev K T, Primatarowa M T and Kamburova R S 2004 *Phys. Rev.* E **70** 066622
Primatarowa M T, Stoychev K T and Kamburova R S 2004 *Phys. Rev.* E **72** 036608
[17] Broderick N G R and Sterke C M 1998 *Phys. Rev.* E **58** 7941
[18] Goodman R H *et al* 2002 *J. Opt. Soc. Am.* B **19** 1635
[19] Mak W C K, Malomed B A and Chu P L 2003 *J. Opt. Soc. Am.* B **20** 725
Mak W C K, Malomed B A and Chu P L 2003 *Phys. Rev.* E **67** 026608
Chen P Y P, Malomed B A and Chu P L 2005 *Phys. Rev.* E **71** 066601
[20] Frantzeskakis D J *et al* 2002 *Phys. Rev.* A **66** 053608
[21] Herring G *et al* 2005 *Phys. Lett.* A **345** 144
Lee C and Brand J 2006 *Europhys. Lett.* **73** 321
Garnier J and Abdullaev F 2006 *Preprint* cond-mat/0605261
[22] Kivshar Y S and Campbell D K 1993 *Phys. Rev.* E **48** 3077